Original Article

Institution of MECHANICAL ENGINEERS

Journal of AEROSPACE ENGINEERING

Proc IMechE Part G:
J Aerospace Engineering
2015, Vol. 229(14) 2634–2645

DOI: 10.1177/0954410015581652
uk.sagepub.com/jaero
SAGE

The composite hierarchical control of multi-link multi-DOF space manipulator based on UDE and improved sliding mode control

ZhongYi Chu[1], JianChao Li[1] and Shan Lu[2]

Abstract

The problem of manipulating objects cooperatively for multi-link multi-degree of freedom space manipulator is very challenging because of the multisource disturbances, including nonlinear coupling, model uncertainties, and external disturbances. To solve this issue, a composite hierarchical control strategy is proposed, which has two layers. In inner layer, uncertainty and disturbance estimator (UDE) is employed to estimate the composite uncertainty that comprises the effect of multisource disturbances and compensate for it, producing the decoupled system. Furthermore, taking the error in UDE estimation into consideration, the chattering–eliminating sliding mode control is designed to suppress it in the outer layer. However, the obtained controller requires the measurement of joint velocities apart from joint positions. To address this issue, a robust velocity observer that employs the UDE-estimated uncertainty is proposed. The notable feature of the proposed design is that it requires neither accurate plant model nor any information about the uncertainty. Also, the design requires only joint position measurements for its implementation. Finally, to demonstrate the effectiveness of the composite hierarchical controller, the simulations of a planar dual-arm manipulator system and the comparisons of the proposed method with the other existing designs are presented.

Keywords

Multi-link multi-DOF, space manipulator, composite hierarchical control, uncertainty and disturbance estimator

Date received: 6 May 2014; accepted: 15 March 2015

Introduction

As space exploration and exploitation expand, the deployment of space structures and satellite launches will increase; thus, the life extension of such systems and the reduction of the associated costs will require extensive inspection, assembly, capture, repair, and maintenance capabilities in orbit. Astronaut extra vehicular activities (EVA) can accomplish most of the in-orbit servicing tasks; however, the cost of human life-supported facilities, the limited time available for the maneuver, and the high risks involved because of different hazards are some serious restrictions for EVA. Space manipulator becomes the best alternative and plays a more important role in future missions.[1,2] As the missions become diversified and complicated and the operation objects become noncooperative, the single-arm space manipulator systems show big disadvantages.[3] To increase the mobility of in-orbit robotic systems, multiple arms with multi-link multi-degree of freedom (DOF) are mounted on spacecraft. Unlike the fix-based robots, the space manipulator has nonlinear coupling between arms and the base body.[4] Thus, issues on manipulating objects cooperatively rise. The issues get further severer when the system is subjected to various model uncertainties and unmeasurable external disturbances, such as inaccuracy of the inertial matrix, joint nonlinear friction, and unknown masses of objects. Hence, to meet the requirements of coordinated manipulation, it is essential to consider the multisource disturbances, including nonlinear coupling, model uncertainties, and external disturbances.[5]

To deal with the composite uncertainty that comprises the effect of all the multisource disturbances, researchers have come up with many useful control

[1]School of Instrument Science and Opto-electronics, Beihang University, Beijing, China
[2]Shanghai Institute of Spaceflight Control Technology, Shanghai Key Laboratory of Aerospace Intelligent Control Technology, Shanghai, China

Corresponding author:
JianChao Li, School of Instrument Science and Opto-electronics, Beihang University, 100191 Beijing, China.
Email: ljc8903@yeah.net

methods, including designs based on proportional derivative (PD) control[6] and adaptive control,[7] as well as neural networks[8] and fuzzy logic control.[9] All these strategies can be used in different situations according to their own specific features. With simple and effective properties, the PD controller does not require any knowledge of the system dynamics, but it cannot follow the desired accuracy and robustness.[6] Designs based on adaptive controller have a good performance on model parametric uncertainties, but show big disadvantages when dealing with nonparametric uncertainties.[10] Although strategies based on neural networks or fuzzy logic controllers can bring about better performance, the complicated controller structure and the acquirement of all states cannot meet the real-time features in engineering applications.[11] Briefly, the above methods have their own issues and could not satisfy the requirements of controlling the system with multisource disturbances absolutely.

One of the best approaches of designing controllers for the system is to estimate the equivalent disturbance acting on the system and compensate for it by augmenting the controller designed for nominal system. Techniques including disturbance observer[12] and unknown input observer[13] have been an active topic to estimate the effect of uncertainties and disturbances. The time delay control (TDC) is one such well-known strategy used for estimation of the system uncertainties.[14] In TDC, a function representing the effect of composite uncertainty is estimated directly using the recent past information, and then, a control is designed using this estimation in such a way to cancel out the effect of the unknown dynamics and the external disturbances. Following the line of TDC and having addressed some issues related to it, the uncertainty and disturbance estimator (UDE) technique, which can overcome the issues of the requirement of knowledge of uncertainty bound, is proposed in Zhong and Rees.[15] In Talole and Phadke,[16] the decoupled dynamics and robustification are achieved by estimating the uncertainties and external unmeasurable disturbances with the UDE and compensating the same. Nevertheless, despite the improved performance, the limitation in UDE leads to estimating error in practice, which significantly affects the performance of the coordinated manipulation for space manipulators; the estimation error of the system has to be dealt with.

With the experience that the lesser the error in estimation, the better the tracking performance, that the greater the ability to suppress the error for the feedback controller, the better the performance of the coordinated manipulation, and that without any of them or with less ability for one of them, the controlling property will deteriorate, the UDE technique and the feedback controller must be considered by synthesis to satisfy the requirements in engineering applications. In many of the feedback control strategies, compared with the PID control, adaptive control, and robust control, the sliding mode control (SMC) is much more effective in suppressing the uncertainties for highly coupled nonlinear systems. Thus, the composite hierarchical control strategy that combines the UDE in feedforward path and SMC in feedback path is proposed synthetically and realized in this paper.

Besides, attention should be paid to the issue that the measurement of joint positions and velocities is required for robotic manipulators. Whereas, joint positions can be accurately measured by good precision encoders, the measurement of joint velocities is often an issue because of the measurement noise. In addition to this, the weight of any additional sensor can also be heavy burdens especially for space manipulators. The estimation of velocities from the positions through approximate differentiation may not be satisfactory, and to obtain the information of velocities from an appropriate observer becomes a better alternative. However, in the presence of model uncertainties, observers based on exact system dynamics suffer from robustness, which is a remaining issue.

This paper focuses on the cooperative control of multi-link multi-DOF space manipulators. The novelty of the work is to propose a composite hierarchical control strategy for multi-link multi-DOF space manipulators dealing against multisource disturbances with UDE and chattering–eliminating SMC, which has two layers. The inner layer includes UDE, which is employed to estimate the composite uncertainty and compensator in feedforward path, thus decoupling the system dynamics. The outer layer takes the error in UDE estimation into consideration and makes full use of the chattering–eliminating SMC that is effective for nonlinear system to suppress it in feedback path. To address the issue that the obtained controller needs the information of joint positions and velocities, a robust velocity observer that employs the UDE-estimated uncertainty is proposed. The proposed design has two notable features: first, it requires neither the accurate plant model nor any information about the uncertainty; second, its implementation only needs the measurement of joint positions. To demonstrate the effectiveness of the composite hierarchical method, simulations of a planar dual-arm manipulator system and comparisons with the other two designs, SMC and PD + UDE, are carried out.

The remaining paper is organized as follows. In Dynamics modeling of the multi-link multi-DOF space manipulator section, the dynamics modeling of multi-link multi-DOF space manipulator system is presented. In The composite hierarchical controller based on UDE and improved SMC section, the composite hierarchical control strategy is introduced, and the closed-loop stability of the overall system is stated in Stability analysis section. The simulations of the dual-arm space manipulator are implemented to verify the proposed controller, and the results are described in Simulations and results section. Eventually, Conclusions section concludes this work.

Dynamics modeling of the multi-link multi-DOF space manipulator

The general configuration of a multi-link multi-DOF space manipulator system and its essential coordinates are shown in Figure 1. Regardless of the effect of orbital dynamics, the motion of the system is considered with respect to an in-orbit inertial frame of reference (XYZ), and the system potential energy is taken as equal to zero.

The dynamics of the complex system can be obtained via Lagrangian formulation[17]

$$\begin{aligned}\mathbf{H}(\boldsymbol{\delta}_0, \boldsymbol{\theta})\ddot{\mathbf{q}} + \mathbf{C}_1(\boldsymbol{\delta}_0, \dot{\boldsymbol{\delta}}_0, \boldsymbol{\theta}, \dot{\boldsymbol{\theta}})\dot{\mathbf{q}} + \mathbf{C}_2(\boldsymbol{\delta}_0, \dot{\boldsymbol{\delta}}_0, \boldsymbol{\theta}, \dot{\boldsymbol{\theta}}) \\ = \mathbf{Q}(\boldsymbol{\delta}_0, \boldsymbol{\theta})\end{aligned} \tag{1}$$

where $\mathbf{H}$ is an $N \times N$ mass matrix, whose elements are given in equation (2); $\mathbf{C}_1$ and $\mathbf{C}_2$ are vectors that contain all the nonlinear velocity terms in a microgravity environment, and decided by equations (3) and (4). Notably, the space manipulators are nonholonomic constraint systems and the derivative of the generalized coordinates are not integral.

$$\begin{aligned}H_{ij} = {} & M \frac{\partial \mathbf{R}_{C_0}}{\partial q_i} \cdot \frac{\partial \mathbf{R}_{C_0}}{\partial q_j} + \frac{{}^0\partial \mathbf{w}_0}{\partial \dot{q}_i} \cdot \Gamma_0 \cdot \frac{{}^0\partial \mathbf{w}_0}{\partial \dot{q}_j} \\ & + \sum_{m=1}^{n} \sum_{k=1}^{N_m} \left(m_k^{(m)} \frac{\partial \mathbf{r}_{C_k}^{(m)}}{\partial q_i} \cdot \frac{\partial \mathbf{r}_{C_k}^{(m)}}{\partial q_j} \right. \\ & \left. + \frac{{}^k\partial \mathbf{w}_k^{(m)}}{\partial \dot{q}_i} \cdot \boldsymbol{\Gamma}_k^{(m)} \frac{{}^k\partial \mathbf{w}_k^{(m)}}{\partial \dot{q}_j} \right) \\ & + \left(\sum_{m=1}^{n} \sum_{k=1}^{N_m} m_k^{(m)} \frac{\partial \mathbf{r}_{C_k}^{(m)}}{\partial q_i} \right) \cdot \frac{\partial \mathbf{R}_{C_0}}{\partial q_j} \\ & + \left(\sum_{m=1}^{n} \sum_{k=1}^{N_m} m_k^{(m)} \frac{\partial \mathbf{r}_{C_k}^{(m)}}{\partial q_j} \right) \cdot \frac{\partial \mathbf{R}_{C_0}}{\partial q_i}\end{aligned} \tag{2}$$

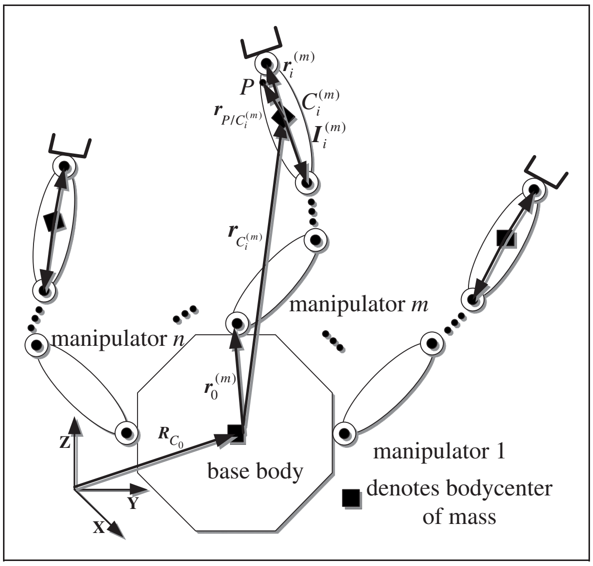

Figure 1. Multi-link multi-DOF space manipulator system.

$$\begin{aligned}C_{1ij} = {} & M \frac{\partial \mathbf{R}_{C_0}}{\partial q_i} \cdot \left(\sum_{s=1}^{N} \frac{\partial^2 \mathbf{R}_{C_0}}{\partial q_s \partial q_j} \dot{q}_s \right) + \frac{{}^0\partial \mathbf{w}_0}{\partial \dot{q}_i} \cdot \boldsymbol{\Gamma}_0 \cdot \frac{{}^0\partial \mathbf{w}_0}{\partial q_j} \\ & + \mathbf{w}_0 \cdot \boldsymbol{\Gamma}_0 \cdot \frac{{}^0\partial^2 \mathbf{w}_0}{\partial \dot{q}_i \partial q_j} + \frac{\partial \mathbf{R}_{C_0}}{\partial q_i} \\ & \cdot \sum_{m=1}^{n} \sum_{k=1}^{N_m} \left(m_k^{(m)} \sum_{s=1}^{N} \frac{\partial^2 \mathbf{r}_{C_k}^{(m)}}{\partial q_s \partial q_j} \dot{q}_s \right) \\ & + \sum_{m=1}^{n} \sum_{k=1}^{N_m} \left(m_k^{(m)} \frac{\partial \mathbf{r}_{C_k}^{(m)}}{\partial q_i} \cdot \left(\sum_{s=1}^{N} \frac{\partial^2 \mathbf{r}_{C_k}^{(m)}}{\partial q_s \partial q_j} \dot{q}_s \right) \right. \\ & \left. + \frac{{}^k\partial \mathbf{w}_k^{(m)}}{\partial \dot{q}_i} \cdot \boldsymbol{\Gamma}_k^{(m)} \cdot \frac{{}^k\partial \mathbf{w}_k^{(m)}}{\partial q_j} + {}^k\mathbf{w}_k^{(m)} \cdot \boldsymbol{\Gamma}_k^{(m)} \cdot \frac{{}^k\partial^2 \mathbf{w}_k^{(m)}}{\partial \dot{q}_s \partial q_j} \right) \\ & + \left(\sum_{s=1}^{N} \frac{\partial^2 \mathbf{R}_{C_0}}{\partial q_s \partial q_j} \dot{q}_s \right) \cdot \sum_{m=1}^{n} \sum_{k=1}^{N_m} \left(m_k^{(m)} \frac{\partial \mathbf{r}_{C_k}^{(m)}}{\partial q_i} \right)\end{aligned} \tag{3}$$

$$C_{2i} = -\left(\mathbf{w}_0 \boldsymbol{\Gamma}_0 \frac{{}^0\partial \mathbf{w}_0}{\partial q_i} + \sum_{m=1}^{n} \sum_{k=1}^{Nm} \mathbf{w}_k^{(m)} \boldsymbol{\Gamma}_k^{(m)} \frac{{}^k\partial \mathbf{w}_k^{(m)}}{\partial q_i} \right) \tag{4}$$

$\mathbf{Q}$ is an $N \times 1$ vector of the generalized forces given on the assumption that all the external forces, except the ones applied on the base body, are zero by the following

$$\mathbf{Q} = \mathbf{J}_Q \tau \tag{5}$$

where $\tau = ({}^0\mathbf{f}_s, {}^0\mathbf{n}_s, \tau_1^{(1)}, \ldots, \tau_{N_1}^{(1)}, \ldots, \tau_1^{(m)}, \ldots, \tau_{N_m}^{(m)}, \ldots, \tau_1^{(n)}, \ldots, \tau_{N_n}^{(n)})^{\mathrm{T}}$; ${}^0\mathbf{f}_s$ and ${}^0\mathbf{n}_s$ are the net force and moment applied on the base body, respectively; $\mathbf{J}_Q$ is an $N \times N$ Jacobian matrix, which is diagonally partitioned. The vector of the generalized coordinate, $\mathbf{q}$ can be chosen as follows

$$\mathbf{q} = \left(\mathbf{q}^{(0)^{\mathrm{T}}}, \mathbf{q}^{(1)^{\mathrm{T}}}, \ldots, \mathbf{q}^{(n)^{\mathrm{T}}} \right)^{\mathrm{T}} \tag{6a}$$

where

$$\mathbf{q}^{(0)} = \left(\mathbf{R}_{C_0}^{\mathrm{T}}, \boldsymbol{\delta}_0^{\mathrm{T}} \right)^{\mathrm{T}} \tag{6b}$$

$$\mathbf{q}^{(m)} = \boldsymbol{\theta}^{(m)} = \left(\theta_1^{(m)}, \ldots, \theta_{N_m}^{(m)} \right)^{\mathrm{T}} \tag{6c}$$

with $\boldsymbol{\theta}_i^{(m)} (i = 1, \ldots, N_m)$ describing the mth manipulator joint angles.

The related symbols in dynamics modeling are described as follows: P is an arbitrary point of the system; n is the number of manipulators; K and N are DOFs of all the manipulators and the whole system, respectively; N_m is the DOF of the mth manipulator; $\mathbf{q}$, $\dot{\mathbf{q}}$, and $\ddot{\mathbf{q}}$ are the vectors of the generalized coordinates, speeds, and accelerations; q_i and $\dot{q}_i$ are the ith element of the vectors of the generalized coordinates and speeds; $\boldsymbol{\delta}_0$ and $\dot{\boldsymbol{\delta}}_0$ are the Euler angles and speeds of the base body; $\mathbf{l}_i^{(m)}$, $\mathbf{r}_i^{(m)}$ are the body-fixed vectors that describe the position of joints i and $i+1$ with respect to C_i, as seen in Figure 1; $\mathbf{w}_0$ and $\mathbf{w}_k^{(m)}$ are the angular velocities of the base body and the kth link of the mth manipulator; $\boldsymbol{\Gamma}_0$, $\boldsymbol{\Gamma}_k^{(m)}$ are the corresponding inertia dyad with respect to their center of the mass; M is the total mass of the system, and $m_k^{(m)}$ represents the mass of the kth link of the mth manipulator; $\mathbf{R}_{C_0}$ describes the vector of the center of the base body mass in inertial frame; $\mathbf{r}_{C_k}^{(m)}$ is the center of the mass of the kth link of the mth manipulator with respect to the center of the base body mass.

The composite hierarchical controller based on UDE and improved SMC

In this section, the two-layer composite hierarchical controller is proposed. To obtain the decoupled system dynamics, the inner layer employs UDE to estimate the composite uncertainty and then compensate for it in feedforward path. The outer layer takes the error of UDE estimation into consideration and makes full use of the chattering–eliminating SMC that is effective for nonlinear system to suppress it in feedback path. To address the issue that the obtained controller needs the information of the joint positions and velocities, a robust velocity observer that employs the UDE-estimated uncertainty is proposed. The symbols interpretation of Figure 2 can be seen in Table 1.

UDE-based decoupling control

Consider the dynamics given by equation (1), because there exists the nonlinear joint coupling and the exact system model is rarely known in practice, it becomes necessary to account for the nonlinear coupling, modeling errors, and external disturbances. In the present work, the inertia matrix, $\mathbf{H}(\boldsymbol{\delta}_0, \boldsymbol{\theta})$, is taken as uncertain with $\mathbf{H} = \mathbf{H}_0 + \Delta\mathbf{H}$ where $\Delta\mathbf{H}$ is its equivalent uncertainty and $\mathbf{H}_0 \triangleq \text{diag}\{H_{11} \ldots H_{ii} \ldots H_{nn}\}$ is a primarily chosen $n \times n$ constant diagonal matrix. Here, H_{ii} is the constant-valued nominal axis inertia term of the ith subsystem and can be generally obtained from the average of the diagonal elements of $\mathbf{H}$ during the motion. Furthermore, the matrix $\mathbf{C}_1$ and $\mathbf{C}_2$ are assumed to be completely unknown. In view of the

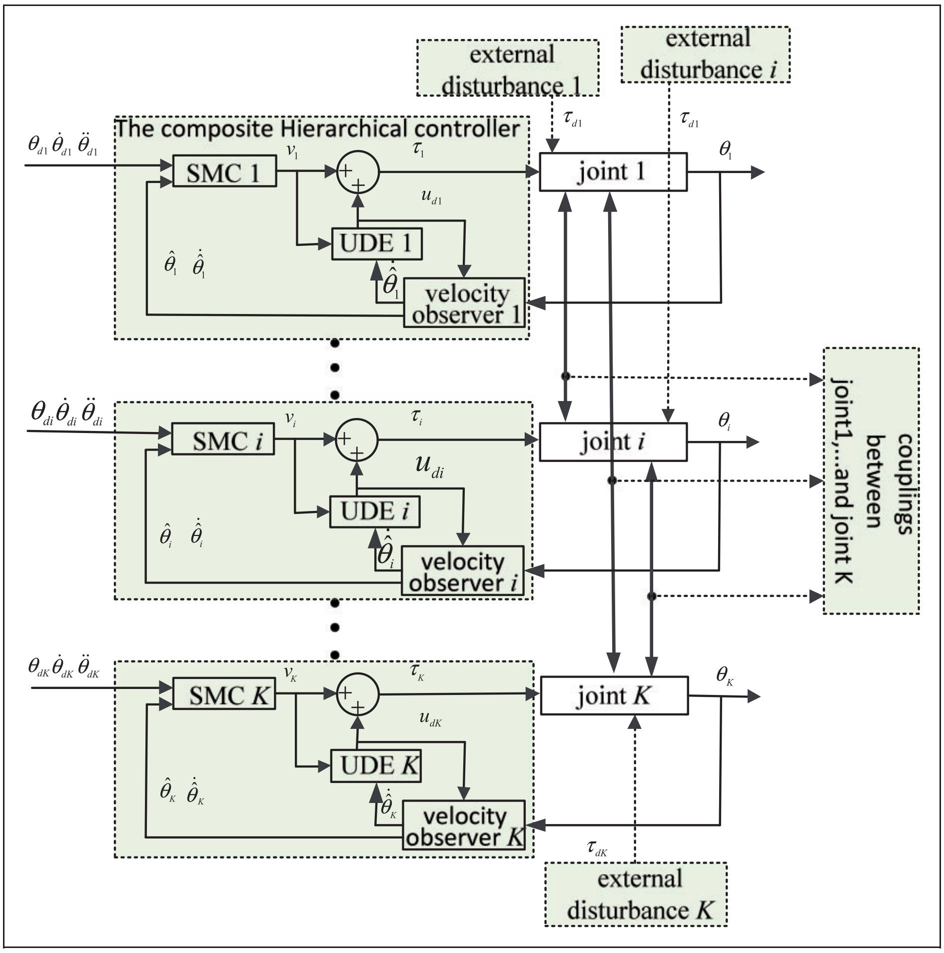

Figure 2. The structure of the composite hierarchical controller.

considered uncertainty and inner joint coupling in $\mathbf{H}$, the dynamics of equation (1) can be rewritten as

$$\ddot{\mathbf{q}} = -\mathbf{H}^{-1}(\mathbf{C}_1\dot{\mathbf{q}} + \mathbf{C}_2) + (\mathbf{H}^{-1} - \mathbf{H}_0^{-1})\mathbf{J}_Q\boldsymbol{\tau} + \mathbf{H}_0^{-1}\mathbf{J}_Q\boldsymbol{\tau} + \mathbf{d}' + \mathbf{d}'' \tag{7}$$

where $\mathbf{d}'$ and $\mathbf{d}''$ represent the effect of the external disturbances and the model nonparametric uncertainty, respectively. Because $\mathbf{C}_1$ and $\mathbf{C}_2$ are assumed as completely unknown, they form a part of the composite uncertainty $\mathbf{d}$ that needs to be estimated, and to this end, the composite uncertainty $\mathbf{d}$ is defined as

$$\mathbf{d} = -\mathbf{H}^{-1}(\mathbf{C}_1\dot{\mathbf{q}} + \mathbf{C}_2) + (\mathbf{H}^{-1} - \mathbf{H}_0{}^{-1})\mathbf{J}_Q\tau + \mathbf{d}' + \mathbf{d}'' \tag{8}$$

In view of equation (8), the dynamics of equation (7) takes the form

$$\ddot{\mathbf{q}} = \mathbf{d} + \mathbf{H}_0{}^{-1}\mathbf{J}_Q\tau \tag{9}$$

where $\mathbf{d} = (d_0, d_1^{(1)}, \ldots, d_{N_1}^{(1)}, \ldots, d_1^{(m)}, \ldots, d_{N_m}^{(m)}, \ldots, d_1^{(n)}, \ldots, d_{N_n}^{(n)})^{\mathrm{T}}$; d_0 is the uncertainty applied on the base body. Noting that $\mathbf{H}_0$ is diagonal, it is straightforward to verify that the dynamics of equation (9) is decoupled. In view of this, the dynamics for the ith link of the mth manipulator can be rewritten as

$$\ddot{\theta}_i^{(m)} = d_i^{(m)} + b_{ii}^{(m)}\tau_i^{(m)}, \quad i = 1, \ldots, N_m; m = 1, \ldots, n \tag{10}$$

where $b_{ii}^{(m)}$ are the corresponding diagonal elements of $\mathbf{H}_0{}^{-1}\mathbf{J}_Q$. To address the issue of the composite uncertainty, the control takes the form as

$$\tau_i^{(m)} = \frac{1}{b_{ii}^{(m)}}\left(u_{di}^{(m)} + v_i^{(m)}\right) \tag{11}$$

where $u_{di}^{(m)}$ is the part of the feedforward controller, which cancels the effect of the composite uncertainty, and $v_i^{(m)}$ is the output of the feedback controller. Substituting equation (11) in equation (10) leads to

$$\ddot{\theta}_i^{(m)} = u_{di}^{(m)} + v_i^{(m)} + d_i^{(m)} \tag{12}$$

one obtains

$$d_i^{(m)} = \ddot{\theta}_i^{(m)} - u_{di}^{(m)} - v_i^{(m)} \tag{13}$$

In view of equation (13) and following the procedure given in Sun et al.,[10] the estimation of $d_i^{(m)}$ is obtained as

$$\hat{d}_i^{(m)} = G_{if}^{(m)}(s)(\ddot{\theta}_i^{(m)} - u_{di}^{(m)} - v_i^{(m)}) \tag{14}$$

where $\hat{d}_i^{(m)}$ is the estimation of $d_i^{(m)}$ and $G_{if}^{(m)}(s)$ is a first-order low pass filter with a time constant of $t_{if}^{(m)}$ to reduce the calculation complexity.

$$G_{if}^{(m)}(s) = \frac{1}{1 + t_{if}^{(m)}s}, \quad i = 1, \ldots, N_m \tag{15}$$

Selecting $u_{di}^{(m)} = -\hat{d}_i^{(m)}$ and substituting equation (15) into equation (14) lead to

$$u_{di}^{(m)} = -G_{if}^{(m)}(s)(\ddot{\theta}_i^{(m)} - u_{di}^{(m)} - v_i^{(m)}) \tag{16}$$

Now, solving for $u_{di}^{(m)}$ leads to

$$u_{di}^{(m)} = -\hat{d}_i^{(m)} = -\frac{G_{if}^{(m)}(s)}{1 - G_{if}^{(m)}(s)}(\ddot{\theta}_i^{(m)} - v_i^{(m)}) = -\frac{1}{t_{if}^{(m)}s}(\ddot{\theta}_i^{(m)} - v_i^{(m)}) \tag{17}$$

Substitution of equation (17) into equation (11) gives the resulting controller in the time domain form

$$\tau_i^{(m)} = \frac{1}{b_{ii}^{(m)}}\left[-\frac{1}{t_{if}^{(m)}}\dot{\theta}_i^{(m)} + v_i^{(m)} + \frac{1}{t_{if}^{(m)}}\int v_i^{(m)}\mathrm{d}t\right], \quad i = 1, \ldots, N_m; m = 1, \ldots, n \tag{18}$$

Note that the more accuracy of the estimation $\hat{d}_i^{(m)}$, the more precise is the compensator $u_{di}^{(m)}$; however, with the limitation of UDE, there always exists error $\tilde{d}_i^{(m)} = d_i^{(m)} - \hat{d}_i^{(m)}$ in practice, and the ability to deal with the error significantly affects the performance of the controller. Therefore, for the perfect controlling performance, control strategies for space manipulators must be designed based on both sides previously mentioned synthetically. After the feedforward controller was obtained, the feedback controller, which employs the SMC to cope with the error, $\tilde{d}_i^{(m)}$, is presented below.

Improved SMC-based disturbance suppression

In this subsection, considering the limitation of UDE's ability in estimating and the compensating in feedforward path, the chattering–eliminating SMC is implemented to deal with the remaining uncertainty, $\tilde{d}_i^{(m)}$ in feedback path.

Considering the decoupled subsystem (equation (10)) and assuming the $\tilde{d}_i^{(m)}$ has a bound

$$|\tilde{d}_i^{(m)}| = |d_i^{(m)} - \hat{d}_i^{(m)}| \leqslant D_i^{(m)} \tag{19}$$

The chattering–eliminating SMC law can be obtained[18]

$$\tau_i^{(m)} = \left(b_{ii}^{(m)}\right)^{-1}\Big[\ddot{\theta}_{di}^{(m)} - \lambda_i^{(m)}(\dot{\theta}_i^{(m)} - \dot{\theta}_{di}^{(m)})$$

$$- \hat{d}_i^{(m)} - k_i^{(m)} \operatorname{sgn}(s_i^{(m)}) \Big] \quad (20)$$

where $\dot{\theta}_{di}^{(m)}$ and $\ddot{\theta}_{di}^{(m)}$ are the desired input velocity and acceleration of the ith link of the mth manipulator; $\dot{\theta}_i^{(m)}$ is the actual velocity of the corresponding joint; $\lambda_i^{(m)}$ $k_i^{(m)}$ are the positive controlling parameters; and $s_i^{(m)}$ is the distance from a sliding surface. Substituting the SMC law (equation (20)) into equation (10) results in the following

$$\ddot{\theta}_i^{(m)} = \ddot{\theta}_{di}^{(m)} - \lambda_i^{(m)}(\dot{\theta}_i^{(m)} - \dot{\theta}_{di}^{(m)}) - k_i^{(m)} \operatorname{sgn}(s_i^{(m)}) \quad (21)$$

Now, defining the output of the SMC as

$$v_i^{(m)} = \ddot{\theta}_{di}^{(m)} - \lambda_i^{(m)}\left(\dot{\theta}_i^{(m)} - \dot{\theta}_{di}^{(m)}\right) - k_i^{(m)} \operatorname{sgn}\left(s_i^{(m)}\right) \quad (22)$$

$$\frac{1}{2}\frac{d}{dt} s_i^{(m)} \leqslant -\eta_i^{(m)} |s_i^{(m)}|, \quad \eta_i^{(m)} > 0 \quad (23)$$

where $\eta_i^{(m)}$ is a factor that indicates the speed of the corresponding state in approaching its sliding surface. In equation (22), $k_i^{(m)}$ is a positive value that must be determined to satisfy the sliding mode condition (equation (23)), and $k_i^{(m)}$ can be obtained using the Filippov's construction of equivalent dynamics[19] by calculating $\dot{s}_i^{(m)} = 0$, which yields the following

$$k_i^{(m)} = D_i^{(m)} + \eta_i^{(m)} \quad (24)$$

If $\eta_i^{(m)}$ can be determined in such a way that is based on the absolute value of the distance from the sliding surface, the speed of the corresponding state becomes lower and reaches zero on the surface; then, the performance will be as desired, and chattering will be substantially alleviated. As a result, $\eta_i^{(m)}$ is chosen

$$\eta_i^{(m)}(t) = \eta_{0i}^{(m)} \left|1 - e^{-|s_i^{(m)}|}\right| \quad (25)$$

The above equation (22) is the final sliding mode controller, and choosing a proper $\eta_{0i}^{(m)}$ in equation (25) will avoid the chattering. Thus, the composite hierarchical controller based on UDE and SMC is given by equations (18) and (22); however, the implementation of the controller requires measurement of joint velocities and positions. The estimation of velocities is obtained by a robust velocity observer.

The robust velocity observer

As is obvious from equation (10), the dynamics are decoupled, and hence, the observer design for the ith link of the mth manipulator is presented. To this end, defining $x_{i1}^{(m)} = \theta_i^{(m)}$ and $x_{i2}^{(m)} = \dot{\theta}_i^{(m)}$, the dynamics of equation (10) can be rewritten in a phase variable state–space model form as

$$\begin{cases} \dot{x}_{i1}^{(m)} = x_{i2}^{(m)} \\ x_{i2}^{(m)} = b_{ii}^{(m)} \tau_i^{(m)} + d_i^{(m)} \\ y_i^{(m)} = x_{i1}^{(m)} \end{cases} \quad (26)$$

Defining the state vector as $\mathbf{x}_{ip}^{(m)} = [\, x_{i1}^{(m)} \quad x_{i2}^{(m)} \,]^{\mathrm{T}} = [\, \theta_i^{(m)} \quad \dot{\theta}_i^{(m)} \,]^{\mathrm{T}}$, the system of equation (26) can be rewritten as

$$\begin{cases} \dot{\mathbf{x}}_{ip}^{(m)} = \mathbf{A}_{ip}^{(m)} \mathbf{x}_{ip}^{(m)} + \mathbf{B}_{ip}^{(m)} \tau_i^{(m)} + \mathbf{B}_{id}^{(m)} d_i^{(m)} \\ y_{ip}^{(m)} = \mathbf{C}_{ip}^{(m)} \mathbf{x}_{ip}^{(m)} \end{cases} \quad (27)$$

where

$$\mathbf{A}_{ip}^{(m)} = \begin{bmatrix} 0 & 1 \\ 0 & 0 \end{bmatrix}; \quad \mathbf{B}_{ip}^{(m)} = \begin{bmatrix} 0 \\ b_{ii}^{(m)} \end{bmatrix}; \quad \mathbf{B}_{id}^{(m)} = \begin{bmatrix} 0 \\ 1 \end{bmatrix};$$
$$\mathbf{C}_{ip}^{(m)} = \begin{bmatrix} 1 & 0 \end{bmatrix} \quad (28)$$

It may be noted that a conventional Luenberger observer will not be able to provide accurate state estimation for the plant of equation (27), owing to the presence of the uncertainty. In view of this, a Luenberger-like observer of the following form is proposed as

$$\begin{cases} \dot{\hat{\mathbf{x}}}_{ip}^{(m)} = \mathbf{A}_{ip}^{(m)} \hat{\mathbf{x}}_{ip}^{(m)} + \mathbf{B}_{ip}^{(m)} \tau_i^{(m)} + \mathbf{B}_{id}^{(m)} \hat{d}_i^{(m)} \\ \qquad + \mathbf{L}_i^{(m)} (y_{ip}^{(m)} - \hat{y}_{ip}^{(m)}) \\ \hat{y}_{ip}^{(m)} = \mathbf{C}_{ip}^{(m)} \hat{\mathbf{x}}_{ip}^{(m)} \end{cases} \quad (29)$$

where $\mathbf{L}_i^{(m)} = \left[\, \beta_{i1}^{(m)} \quad \beta_{i2}^{(m)} \,\right]^{\mathrm{T}}$ is the observer gain vector and $\hat{\mathbf{x}}_{ip}^{(m)} = [\, \hat{x}_{i1}^{(m)} \quad \hat{x}_{i2}^{(m)} \,]^{\mathrm{T}} = [\, \hat{\theta}_i^{(m)} \quad \dot{\hat{\theta}}_i^{(m)} \,]^{\mathrm{T}}$. Because the uncertainty is the same as present in equation (10), the UDE-estimated uncertainty is also used in the observer (equation (29)). It may be noted that the proposed velocity observer does not need an accurate plant model and is robust.

Stability analysis

From the above analysis, the control from equation (11) can be rewritten as

$$\tau_i^{(m)} = \left(b_{ii}^{(m)}\right)^{-1} \Big[\ddot{\theta}_{di}^{(m)} - \lambda_i^{(m)} (\dot{\hat{\theta}}_i^{(m)} - \dot{\theta}_{di}^{(m)})$$
$$- k_i^{(m)} \operatorname{sgn}(s_i^{(m)}) - \hat{d}_i^{(m)} \Big] \quad (30)$$

Defining the reference state vector $\mathbf{R}_i^{(m)} = [\, \hat{\theta}_{di}^{(m)} \quad \dot{\hat{\theta}}_{di}^{(m)} \,]^{\mathrm{T}}$ and the state feedback gain vector $\mathbf{K}_{ip}^{(m)} = [\, 0 \quad \frac{\lambda_i^{(m)}}{b_{ii}^{(m)}} \,]$, the control (equation (30)) is rewritten as

$$\tau_i^{(m)} = -\mathbf{K}_{ip}^{(m)}\hat{\mathbf{x}}_{ip}^{(m)} + \mathbf{K}_{ip}^{(m)}\mathbf{R}_i^{(m)} + \frac{1}{b_{ii}^{(m)}}\ddot{\theta}_{di}^{(m)} - \frac{k_i^{(m)}}{b_{ii}^{(m)}}\operatorname{sgn}(s_i^{(m)}) - \frac{1}{b_{ii}^{(m)}}\hat{d}_i^{(m)} \tag{31}$$

It is obviously to show that the dynamics of reference state vector, $\mathbf{R}_i^{(m)}$, can be rewritten as

$$\dot{\mathbf{R}}_i^{(m)} = \mathbf{A}_{ip}^{(m)}\mathbf{R}_i^{(m)} + \mathbf{B}_{id}^{(m)}\ddot{\theta}_{di}^{(m)} \tag{32}$$

Defining the state tracking error $\mathbf{e}_{ic}^{(m)} = \mathbf{R}_i^{(m)} - \mathbf{x}_{ip}^{(m)}$ and from equations (24), (25), (30)–(32), the state tracking error dynamics can be deduced as

$$\dot{\mathbf{e}}_{ic}^{(m)} = (\mathbf{A}_{ip}^{(m)} - \mathbf{B}_{ip}^{(m)}\mathbf{K}_{ip}^{(m)})\mathbf{e}_{ic}^{(m)} - \mathbf{B}_{ip}^{(m)}\mathbf{K}_{ip}^{(m)}\mathbf{e}_{io}^{(m)} - \mathbf{B}_{id}^{(m)}(D_i^{(m)}\operatorname{sgn}(s_i^{(m)}) - \tilde{d}_i^{(m)}) + \mathbf{B}_{id}^{(m)}\eta_{0i}^{(m)}|1 - e^{-|s_i^{(m)}|}|\operatorname{sgn}(s_i^{(m)}) \tag{33}$$

where $\tilde{d}_i^{(m)} = d_i^{(m)} - \hat{d}_i^{(m)}$ is the uncertainty estimation error and $\mathbf{e}_{io}^{(m)} = \mathbf{x}_{ip}^{(m)} - \hat{\mathbf{x}}_{ip}^{(m)}$ is the observer state estimation error vector. The observer error dynamics can be obtained by subtracting equation (29) from equation (27) as

$$\dot{\mathbf{e}}_{io}^{(m)} = (\mathbf{A}_{ip}^{(m)} - \mathbf{L}_i^{(m)}\mathbf{C}_{ip}^{(m)})\mathbf{e}_{io}^{(m)} + \mathbf{B}_{id}^{(m)}\tilde{d}_i^{(m)} \tag{34}$$

From equations (13) and (14), the estimation of the uncertainty, $d_i^{(m)}$, is given as

$$\hat{d}_i^{(m)} = G_{if}^{(m)}(s)d_i^{(m)} \tag{35}$$

and by processing equation (13), the uncertainty estimation error dynamics is obtained

$$\dot{\tilde{d}}_i^{(m)} = -\frac{1}{t_{if}}\tilde{d}_i^{(m)} + \dot{d}_i^{(m)} \tag{36}$$

Combining equations (33), (34), and (36) yields the following error dynamics for the closed-loop subsystem of the ith link of the mth manipulator

$$\begin{bmatrix}\dot{\mathbf{e}}_{ic}^{(m)}\\ \dot{\mathbf{e}}_{io}^{(m)}\\ \dot{\tilde{d}}_i^{(m)}\end{bmatrix} = \begin{bmatrix}(\mathbf{A}_{ip}^{(m)} - \mathbf{B}_{ip}^{(m)}\mathbf{K}_{ip}^{(m)}) & -(\mathbf{B}_{ip}^{(m)}\mathbf{K}_{ip}^{(m)}) & 0\\ 0 & (\mathbf{A}_{ip}^{(m)} - \mathbf{L}_i^{(m)}\mathbf{C}_{ip}^{(m)}) & \mathbf{B}_{id}^{(m)}\\ 0 & 0 & -\frac{1}{t_{if}}\end{bmatrix} \times \begin{bmatrix}\mathbf{e}_{ic}^{(m)}\\ \mathbf{e}_{io}^{(m)}\\ \tilde{d}_i^{(m)}\end{bmatrix} + \begin{bmatrix}0\\0\\1\end{bmatrix}\dot{d}_i^{(m)} + \begin{bmatrix}\mathbf{B}_{id}^{(m)}\\0\\0\end{bmatrix}\left(\left(D_i^{(m)}\operatorname{sgn}(s_i^{(m)}) - \tilde{d}_i^{(m)}\right) + \eta_{0i}^{(m)}|1 - e^{-|s_i^{(m)}|}|\operatorname{sgn}(s_i^{(m)})\right) \tag{37}$$

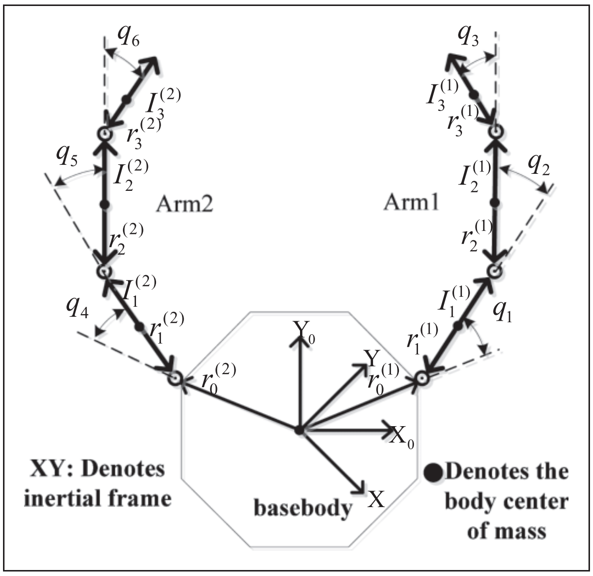

Figure 3. The planar dual-arm manipulator system.

Table 1. Symbols interpretation of Figure 2.

K	The joint number of the multi-arm multi-link space manipulator
$\theta_{di}, \dot{\theta}_{di}, \ddot{\theta}_{di}$ $i = 1, \ldots, K$	The desired position, speeds, and acceleration of the ith joint, separately
$\hat{\theta}_i, \dot{\hat{\theta}}_i, i = 1, \ldots, K$	The estimation of position, θ_i, and speed, $\dot{\theta}_i$ of the ith joint, separately
$v_i, i = 1, \ldots, K$	The output of the feedback controller
$\tau_i, i = 1, \ldots, K$	The designed control force
$u_{id}, i = 1, \ldots, K$	The part of the feedforward controller, which cancels the effect of the composite uncertainty
$\tau_{di}, i = 1, \ldots, K$	The external disturbance of the ith joint

Table 2. Control parameters of SMC + UDE.

Parameters	Joint 1	Joint 2	Joint 3	Joint 4	Joint 5	Joint 6
λ	7.0	6.5	6.5	8.0	7.0	7.0
η_0	0.1	0.1	0.1	0.1	0.1	0.1
Poles	45.90	15.50	20.55	30.70	20.65	20.65
D	0.005	0.005	0.005	0.005	0.005	0.005

Note: SMC, sliding mode control; UDE, uncertainty and disturbance estimator.

For convenient analysis, define $\ell_i^{(m)} = (D_i^{(m)}\mathrm{sgn}(s_i^{(m)}) - \tilde{d}_i^{(m)}) + \eta_{0i}^{(m)}|1 - e^{-|s_i^{(m)}|}|\mathrm{sgn}(s_i^{(m)})$. With the corresponding state arriving its sliding surface and choosing the proper upper bound $D_i^{(m)}$, $\ell_i^{(m)}$ becomes an infinitesimal, and equation (37) can be rewritten as

$$\begin{bmatrix} \dot{\mathbf{e}}_{ic}^{(m)} \\ \dot{\mathbf{e}}_{io}^{(m)} \\ \dot{\tilde{d}}_i^{(m)} \end{bmatrix} = \begin{bmatrix} (\mathbf{A}_{ip}^{(m)} - \mathbf{B}_{ip}^{(m)}\mathbf{K}_{ip}^{(m)}) & -(\mathbf{B}_{ip}^{(m)}\mathbf{K}_{ip}^{(m)}) & 0 \\ 0 & (\mathbf{A}_{ip}^{(m)} - \mathbf{L}_i^{(m)}\mathbf{C}_{ip}^{(m)}) & \mathbf{B}_{id}^{(m)} \\ 0 & 0 & -\frac{1}{t_{if}} \end{bmatrix} \times \begin{bmatrix} \mathbf{e}_{ic}^{(m)} \\ \mathbf{e}_{io}^{(m)} \\ \tilde{d}_i^{(m)} \end{bmatrix} + \begin{bmatrix} 0 \\ 0 \\ 1 \end{bmatrix} \dot{d}_i^{(m)} + \begin{bmatrix} \xi_i^{(m)} \\ 0 \\ 0 \end{bmatrix} \tag{38}$$

where $\xi_i^{(m)}$ is also an infinitesimal. From equation (38), the subsystem matrix being in a block triangular form, it can be easily verified that the eigenvalues of the subsystem matrix are given by

$$\left|sI - (\mathbf{A}_{ip}^{(m)} - \mathbf{B}_{ip}^{(m)}\mathbf{K}_{ip}^{(m)})\right| \left|sI - \left(\mathbf{A}_{ip}^{(m)} - \mathbf{L}_i^{(m)}\mathbf{C}_{ip}^{(m)}\right)\right| \times \left|s - \left(-\frac{1}{t_{if}}\right)\right| = 0 \tag{39}$$

Noting that the pair $(\mathbf{A}_{ip}^{(m)}, \mathbf{B}_{ip}^{(m)})$ is controllable and the pair $(\mathbf{A}_{ip}^{(m)}, \mathbf{C}_{ip}^{(m)})$ is observable, the controller gain, $\mathbf{K}_{ip}^{(m)}$, and the observer gain, $\mathbf{L}_i^{(m)}$, can be chosen appropriately with $t_{if} > 0$ to ensure state ability for error dynamics. As the error dynamics is driven by $\dot{d}_i^{(m)}$, it is obvious that, for bounded $|\dot{d}_i^{(m)}|$, bounded input bounded output stability is assured. If the rate of changed of uncertainty $\dot{d}_i^{(m)} \approx 0$, then the error dynamics for subsystem of the ith link of the mth manipulator is asymptotically stable. With the error dynamics of all the subsystems being asymptotically stable, the overall control system is asymptotically stable.

Simulations and results

In this section, the planar dual-arm manipulator system, shown in Figure 3, which works in free-floating mode, is implemented to verify the effect of the proposed controller, and the results are presented. The configuration parameters of the system used in the simulation are obtained from Guo and Chen.[20] The controller gains required in equation (22) are listed in Table 2, values of $t_{if}^{(m)}$ are all chosen as 0.05 s and the observer gains, $\mathbf{L}_i^{(m)}$, are obtained by placing the observer poles as shown in Table 2. The initial conditions for the observer are taken as zero. In simulations, uncertainty is introduced by considering $m_i^{(m)}$'s uncertainty by +20% of their respective nominal values. Actuator saturation limits of the $\tau_i^{(m)}$ are ± 10 N, and a load disturbance torque of +5% of the maximum input torques is considered. Furthermore, the model nonparametric uncertainty is taken as

$$\mathbf{d}'' = 0.01[3\sin(20\pi q_1); \sin(20\pi q_2); 0.3\sin(20\pi q_3); 3\sin(20\pi q_4); \sin(20\pi q_5); 0.3\sin(20\pi q_6)] \tag{40}$$

The desired position trajectories are taken as sinusoids and cosinsoids, shown in Figure 4. The values of $b_{ii}^{(m)}$ can be obtained from equation (10). Parameters of SMC and PD + UDE are listed in Tables 3 and 4. Observer poles in PD + UDE are the same as those of SMC + UDE. With these data, simulations are carried out, and the comparisons are presented in Figure 5. For simple description, SMC, PD + UDE, and SMC + UDE are numbered as 1, 2, and 3, respectively.

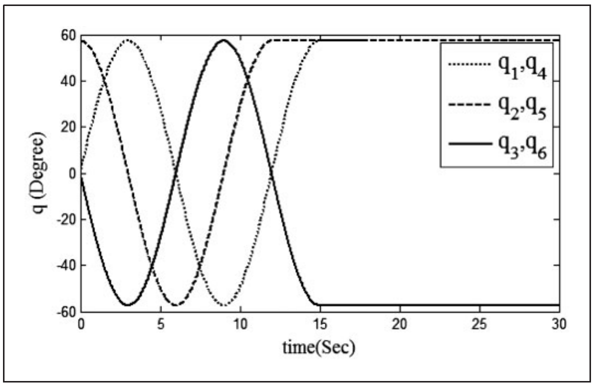

Figure 4. The desired input signals of joints 1–6.

Table 3. Control parameters of SMC.

Parameters	Joint 1	Joint 2	Joint 3	Joint 4	Joint 5	Joint 6
λ	25.0	25.0	30.0	25.0	25.0	20.0
η_0	1.5	1.5	1.5	1.5	1.5	1.5

Note: SMC, sliding mode control.

Table 4. Control parameters of PD + UDE.

Parameters	Joint 1	Joint 2	Joint 3	Joint 4	Joint 5	Joint 6
k_p	12	13	13	13	12	13
k_d	15	15	15	15	15	15

Note: PD, proportional derivative; UDE, uncertainty and disturbance estimator.

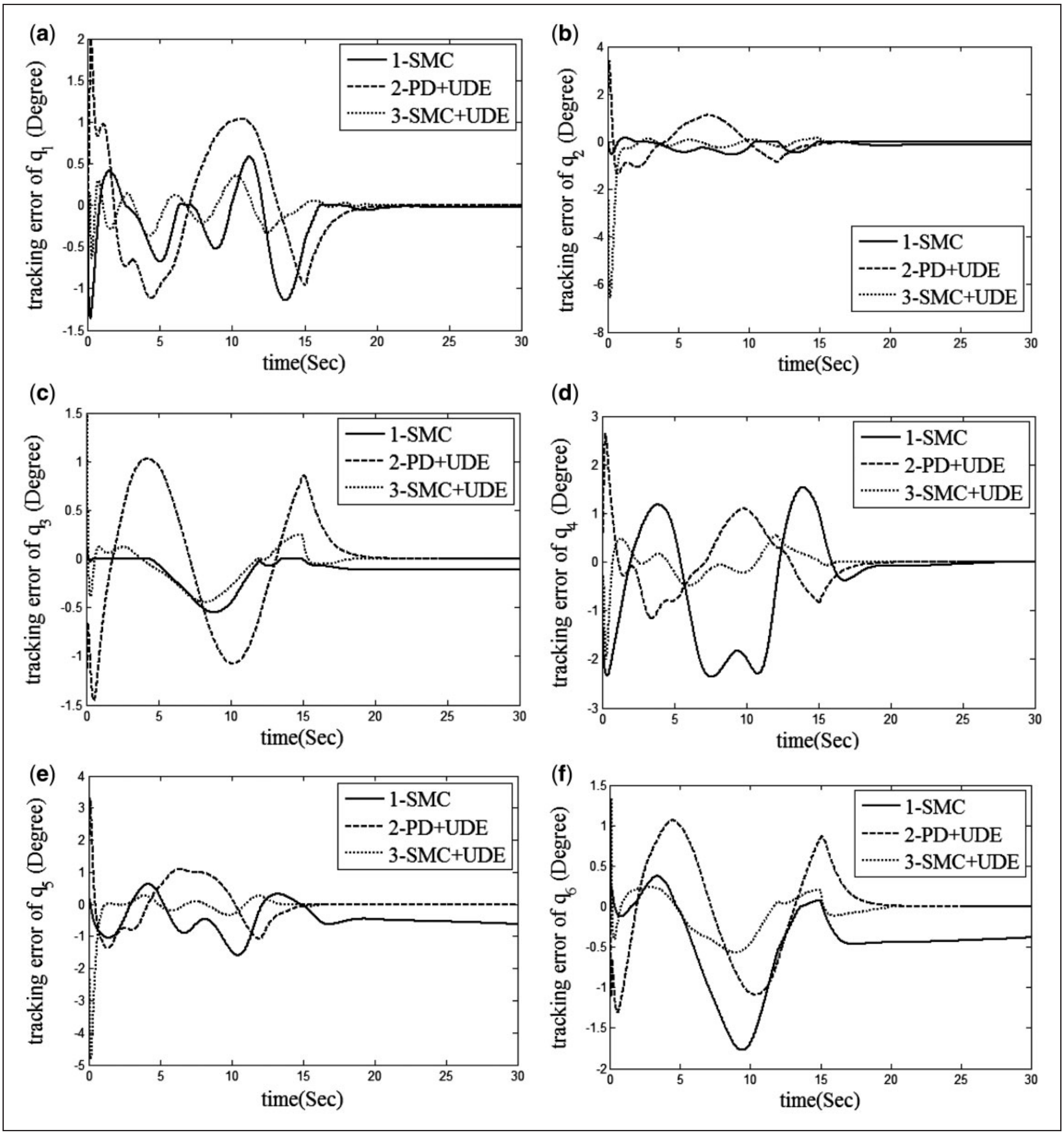

Figure 5. The performance comparison of SMC + UDE and the other two.

From Figure 5, it can be seen that the tracking error is nonzero because of the nonconstant reference input, which results in $\dot{d}_i^{(m)} \neq 0$ in equation (38). Also, it can be obviously observed that controller 1 often has steady-state error in position tracking; however, controllers 2 and 3 have resulted in better tracking performance without steady-state error. To assess performances in dynamic trajectory tracking, the ratios of the absolute value of the maximum magnitude of tracking error to the amplitude of the reference signal for all the three designs are presented in Table 5. It can be noticed that the values of ratios for controller 1 are higher compared with that of controller 3, while the values of ratios for controller 2 are also

Table 5. Comparative performance of SMC, SMC + UDE, and PD + UDE in dynamic trajectory tracking.

Controller	Joint 1	Joint 2	Joint 3	Joint 4	Joint 5	Joint 6
1. SMC	2.10%	0.87%	0.96%	4.10%	2.62%	3.14%
2. PD + UDE	1.75%	1.92%	5.50%	4.71%	2.23%	2.10%
3. SMC + UDE	0.70%	0.35%	0.44%	2.27%	0.35%	0.23%

Note: PD, proportional derivative; SMC, sliding mode control; UDE, uncertainty and disturbance estimator.

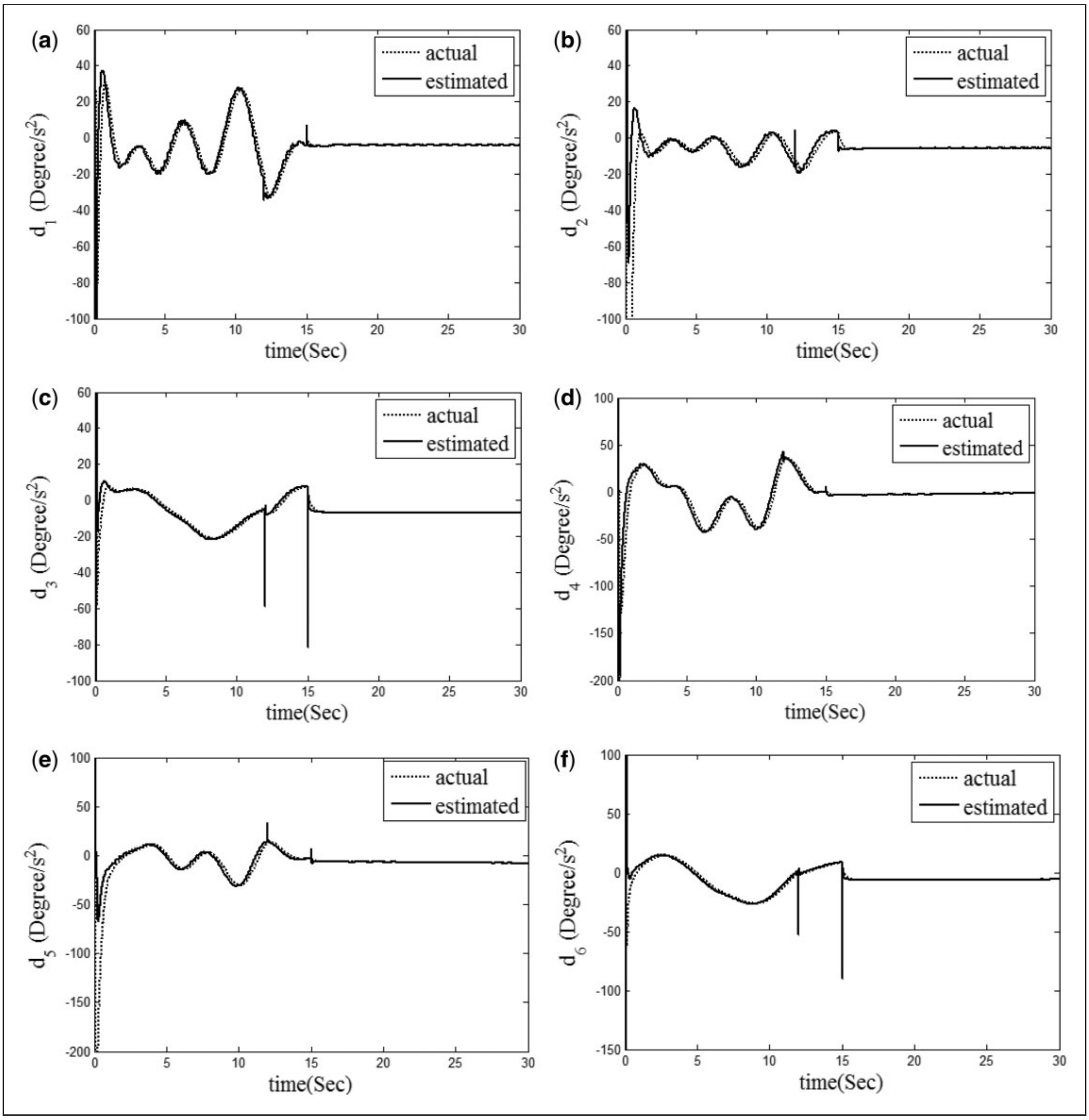

Figure 6. The performance of uncertainty and disturbance estimation.

higher than that of controller 3. To be more specific, on one hand, the introduction of UDE brings about much better performance with zero steady-state error and smaller ratio, which can be inferred from the comparison of controllers 1 and 3. On the other hand, in the comparison of controllers 2 and 3, taking the error of UDE into consideration produces smaller trajectory tracking error. In a word, the proposed composite hierarchical controller achieves highly satisfactory performance and can be used to manipulate objects cooperatively for multi-link multi-DOF space manipulator.

Besides, the proposed composite hierarchical controller offers certain distinct advantages. First, with the UDE technique, the proposed method does not need knowledge of accurate bounds of uncertainties, because all the uncertainties and disturbances are estimated using UDE technique, as shown in Figure 6. Note that with the sudden stop of all the joints, the momentary impacts appear naturally in Figure 6(a) to (f). Second, as seen from Figure 7, the information of joint velocities can be obtained by a robust velocity observer, and the implementation of controller 3 needs joint position only.

Conclusions

In this paper, to meet the requirements in coordinated manipulation for space manipulator, a composite hierarchical control approach is proposed. To deal

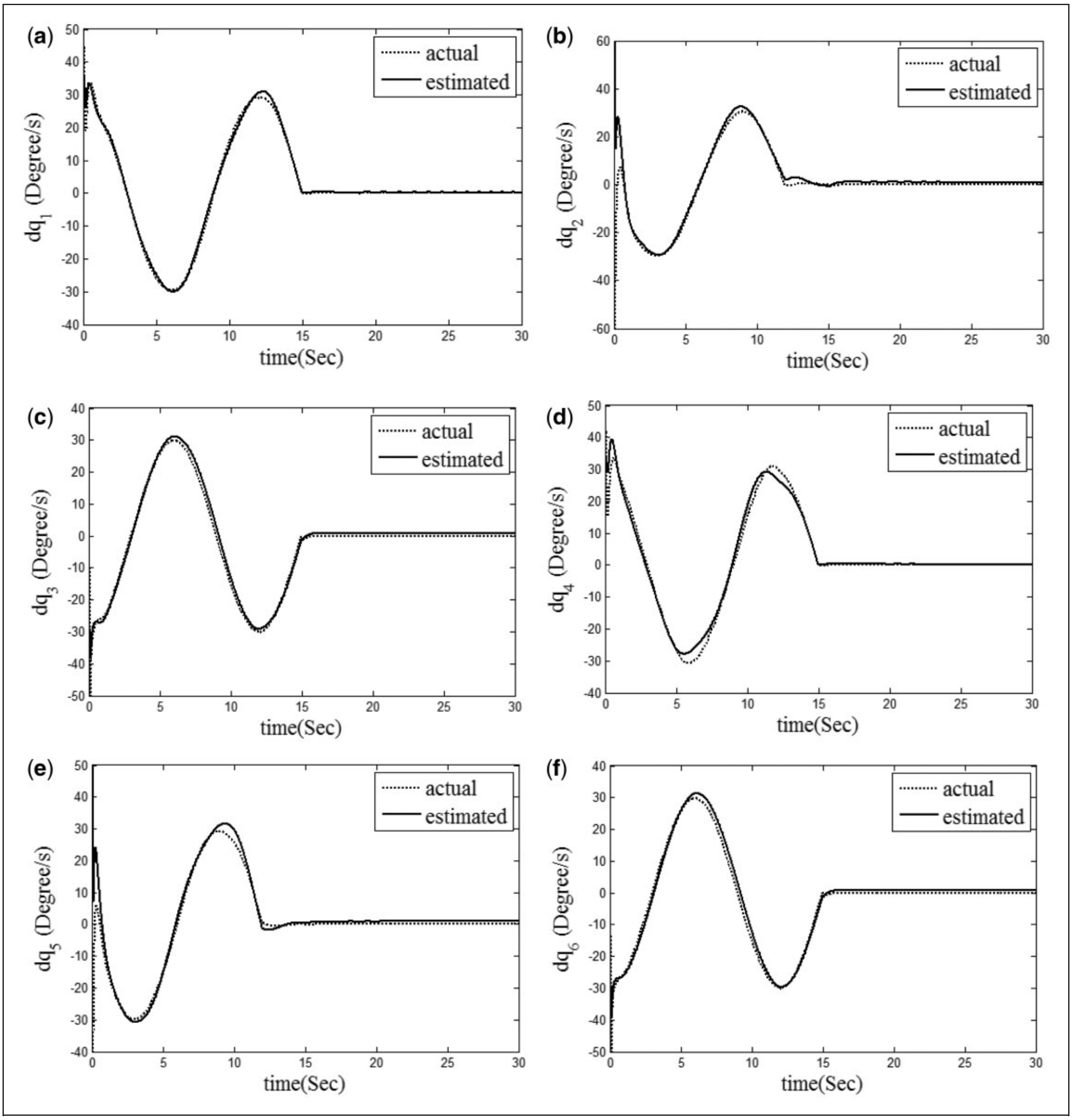

Figure 7. The performance of velocity observers.

with the composite uncertainty that comprises the effect of all the multisource disturbances, the control strategy is designed with two layers: the inner layer includes UDE and compensator in feedforward path, and the outer layer includes the chattering–eliminating SMC in feedback path, having considered the error in UDE estimation. As the resulting controller requires joint velocities apart from joint positions, a robust velocity observer is proposed to provide the estimation of joint velocities. The notable feature of the proposed design is that it requires neither the accurate plant model nor any information about the uncertainty. The simulations of a planar dual-arm manipulator system are implemented to verify the effectiveness of the proposed method, and the comparisons of its performance with SMC and PD + UDE are presented.

Funding

This work was supported by National Science Foundation of China, the contract numbers are 51375034 and 61327809.

Conflict of interests

None declared.

References

1. Moosavian SAA and Papadopoulos E. Free-flying robots in space: an overview of dynamics modeling, planning and control. *Robotica* 2007; 25: 537–547.

2. Zhao JL, Wu JN, Yan SZ, et al. Dynamic modeling and motion precision analysis of spacecraft manipulator with harmonic drive considering the alternative thermal field in orbit. *Proc IMechE, Part G: J Aerospace Engineering* 2014; 0954410014527267.
3. Liang B, Du XD and Li C. Advances in space robot on-orbit servicing for non-cooperative spacecraft. *Robot* 2012; 34: 242–256.
4. Ellery A. An engineering approach to the dynamic control of space robotic on-orbit servicers. *Proc IMechE, Part G: J Aerospace Engineering* 2004; 218: 79–98.
5. Moosavian SAA and Ashtiani HR. Cooperation of robotic manipulators using non-model-based multiple impedance control. *Industr Robot: Int J* 2008; 35: 549–558.
6. Astrom KJ and Tore H. *Advanced PID control*. Triangle Park, NC: The Instrumentation, Systems, and Automation Society, 2005.
7. Cong PC, Lan YF and Zhang X. Adaptive control of dual-arm space manipulator capturing object. *Proc IMechE, Part G: J Aerospace Engineering* 2013; 227: 992–999.
8. Hu XP, Zhang WH and Ji XM. Adaptive robust control free-floating space robotic manipulators based on RBF neural network. *Int J Comp Sci Iss* 2012; 9: 158–163.
9. Fateh MM. Robust fuzzy control of electrical manipulators. *J Intell Robot Syst* 2010; 60: 415–434.
10. Sun T, Pei H, Pan Y, et al. Neural network-based sliding mode adaptive control for robot manipulators. *Neurocomputing* 2011; 74: 2377–2384.
11. Chu ZY, Cui J and Sun FC. Fuzzy adaptive disturbance-observer based robust tracking control of electrically driven free-floating space manipulator. *IEEE Syst J* 2014; 8: 343–352.
12. Kolhe JP, Shaheed M, Chandar TS, et al. Robust control of robot manipulators based on uncertainty and disturbance estimation. *Int J Rob Nonlin Contr* 2013; 23: 104–122.
13. Takahashi RHC and Peres PLD. Unknown input observers for uncertain systems: a unifying approach and enhancements. In: *Proceedings of the 35th conference on decision and control*. Kobe, Japan, 199611–13 December.
14. Koucef-Toumi K and Ito O. A time delay controller for systems with unknown dynamics. *Trans ASME J Dyn Syst Measur Contr* 1990; 112: 133–142.
15. Zhong QC and Rees D. Control of uncertain LTI systems based on an uncertainty and disturbance estimator. *Trans ASME J Dyn Syst Measur Contr* 2004; 126: 905–910.
16. Talole SE and Phadke SB. Robust input–output linearisation using uncertainty and disturbance estimation. *Int J Contr* 2009; 82: 1794–1803.
17. Moosavian SAA and Papadopoulos E. Explicit dynamics of space free-flyers with multiple manipulators via SPACEMAPLE. *Adv Robot* 2004; 18: 223–244.
18. Khaloozadeh H and Homaeinejad MR. Real-time regulated sliding mode controller design of multiple manipulator space free-flying robot. *J Mech Sci Technol* 2010; 24: 1337–1351.
19. Slotine JJE and Li W. *Applied nonlinear control*. Englewood Cliffs, New Jersey: Prentice Hall, 1991.
20. Guo YS and Chen L. Bi-directional approach for motion planning of dual-arm space robot systems. *China J Space Sci* 2005; 25: 564–568.